Front. Phys., 2013, 8(3): 257–269
DOI 10.1007/s11467-013-0295-y

REVIEW ARTICLE

Results on non-SUSY searches for physics beyond standard model in *pp* collisions at CMS

Adrian Perieanu[†], **on behalf of the CMS Collaboration**

Physikalisches Institut B, RWTH-Aachen, Germany

E-mail: [†]*Adrian.Perieanu@cern.ch*

Received December 10, 2012; accepted January 14, 2013

In this paper a review of the results on searches for physics beyond the standard model in pp collisions with the CMS experiment at $\sqrt{s} = 7$ and 8 TeV is presented. Aspects of the analyses and their achieved limits on Z'- and W'-bosons, heavy neutrino, 4^{th} generation, leptoquarks as well as extra dimensions will be covered.

Keywords beyond standard model, gauge bosons, leptoquarks, extra dimensions

PACS numbers 14.70.-e, 12.60.-i, 04.50.-h, 14.65.Jk, 95.35.+d, 04.70.Dy

Contents

1 Introduction

In contrast with the supersymmetry (SUSY) [1, 2] searches where a certain benchmark of the model is looked for, the non-SUSY searches for physics beyond the predictions of the standard model (SM) have no predefined path. Often the results are given as model independent as possible letting the various theoretical models to confront their predictions with the observed results in certain final states, e.g., $\mu^+\mu^-$. In order to improve the searches sensitivity, the CMS detector and the physics objects, e.g., tau-lepton candidates, need to be well understood. This section presents a short overview of the CMS apparatus and the performance in reconstructing the objects needed in various analyses. In this paper the natural units system is used, $\hbar = c = 1$.

The central feature of the CMS is a superconducting solenoid, providing a 3.8 T magnetic field. Within the field volume are the silicon pixel and strip tracker, the crystal electromagnetic calorimeter (ECAL) and the brass/scintillator hadron calorimeter (HCAL). The tracks can be reconstructed with transverse momentum (p_T) as low as 100 MeV and a p_T resolution of 1% at 100 GeV. The energy resolution achieved by ECAL is $3\%/\sqrt{E_T/\text{GeV}}$ while in HCAL it is $100\%/\sqrt{E_T/\text{GeV}}$. Muons are measured in gas-ionization detectors embedded in the steel return yoke. A detailed description of the CMS detector can be found elsewhere [3].

The muons are reconstructed starting from the tracks found in the Muon System. These tracks are then matched with the ones from the pixel and strip tracking system forming the global tracks of the muons. The CMS acceptance can be described with the pseudo-rapidity $\eta = -\ln(\theta/2)$, where θ is the polar angle. The muons can be reconstructed up to $\eta = 2.4$ and the achieved resolution of the transverse momentum, p_T, is $0.015\% \cdot p_T \oplus 0.5\%$. A complete overview of the muon reconstruction performance is given in Ref. [4].

The electron candidates in CMS combine the energy from ECAL clusters with tracks reconstructed by the Gaussian Sum Filter (GSF) algorithm [5]. They can be reconstructed in the $|\eta| < 1.4442$ and $1.556 < |\eta| < 2.5$ range with a transverse energy resolu-

tion of $3\%/\sqrt{E_T/\mathrm{GeV}}$.

The tau-lepton candidates are reconstructed with the particle flow algorithm [7]. The identification is performed using their leptonic decay products, electrons or muons, and the Hadron Plus Strips (HPS) algorithm [6] for hadronic decays. The particle-flow charged hadron candidates are combined with clusters of nearby photons. The photons, produced in the π^0 decays, are clustered (η, φ)-strips accounting also for the electrons coming from their conversion. The tau candidates can be reconstructed in CMS detector up to $\eta = 2.3$ and their energy scale is known with a precision of 3%.

Another important ingredient in the search for physics beyond SM are the jets. The partons can fragment into jets that can be reconstructed within the CMS detector acceptance. In case of b-quarks, the jets can be identified by an appropriate b-tagging algorithm [8]. The jets are reconstructed using the *anti-*κ_T jet selection algorithm [9] with a radius of 0.5. The particle flow technique is used to reconstruct and identify all stable particles within the detector, performing the needed cleaning of reconstructed jets in order to determine the missing energy in the transverse plane, E_T^{miss}, in the event. The E_T^{miss} is defined as the negative vector sum of all particle candidates and jets reconstructed with the PF algorithm.

The various pile-up conditions were considered and the physics objects were corrected accordingly [10].

2 Z'- and W'-bosons searches

The existence of narrow resonances at the TeV scale is foreseen in many theoretical models predicting physics beyond the SM. Two of these models, Sequential Standard Model with Z_{SSM} having a SM-like couplings [11] and the Z_Ψ expected in grand unied theories [12] foresee for a mass of 1 TeV widths of 30 and 7 GeV, respectively.

A search for this type of narrow resonances in the dilepton (e^+e^-, $\mu^+\mu^-$) mass spectra using proton-proton collision data collected with CMS at $\sqrt{s} = 7$ and 8 TeV was performed [13]. Data corresponding to 5.3 fb^{-1} integrated luminosity at 7 TeV and to 4.1 fb^{-1} at 8 TeV were analysed. The events were selected using double lepton triggers, while the leptons had to be isolated and have $p_T > 35$ GeV for electrons, and 45 GeV for muons. The main background contributions are primarily due to SM processes as Drell–Yan and $t\bar{t}$ production. Other prompt leptons that can contribute come from double boson production (WW, WZ and ZZ) and from jets misreconstructed as leptons.

In Fig. 1 the dimuon spectrum observed in the analysed data at $\sqrt{s} = 8$ TeV is presented. The corresponding SM background contributions derived using Monte Carlo simulations (MC) describe the data and no excess is observed. Therefore limits are calculated with an unbinned likelihood fit of the dilepton mass. The obtained limits are expressed as a function of the ratio: $R_\sigma = \frac{pp\to Z'+X\to\ell\ell+X}{pp\to Z+X\to\ell\ell+X}$ with $\ell = e, \mu$. This ratio reduces the dependence on the detector effects as acceptance, trigger, selection efficiencies, and eliminates the systematic uncertainty from the integrated luminosity measurement.

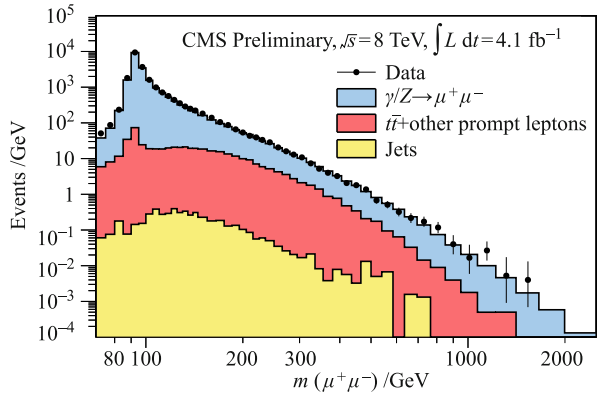

Fig. 1 The $\mu^+\mu^-$ invariant mass distribution for $\sqrt{s} = 8$ TeV analysed data and the corresponding SM background contributions normalized to their cross-sections.

The achieved limits are presented in Fig. 2 together with the model predictions. One can exclude with 95% C.L. the Z'_{SSM} with standard model-like couplings below 2590 GeV and the superstring-inspired Z'_Ψ below 2260 GeV.

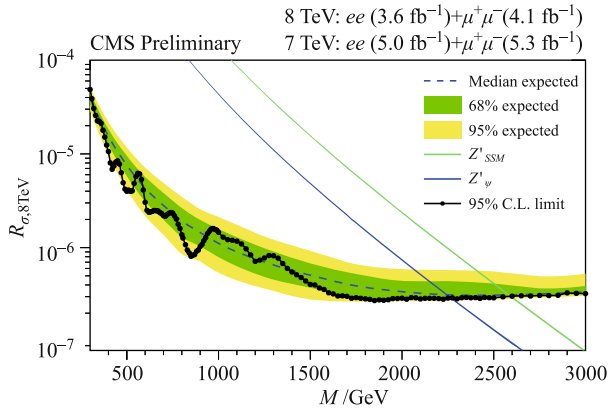

Fig. 2 The expected and observed upper limits on the ratio of the cross-section times branching fraction into dileptons for Z'_{SSM} and Z'_Ψ production to the one for Standard Model Z^0 production. The limits and model predictions are given as a function of the resonance mass. The green and yellow bands correspond to one and two standard deviations, respectively.

A similar search was performed also for a new heavy gauge boson W'. The results of this search can be also interpreted from the perspective of universal extra dimensions (UED) with bulk fermions, or split-UED [14, 15]. The model is based on extended space-time with

an additional fifth dimension where the SM particles are accompanied by corresponding Kaluza–Klein (KK) partners.

For the this search [16] single lepton events were selected with $p_T > 90$ GeV electrons, and 45 GeV muons. In order to enhance events with topology similar with the one from the W-boson SM production, the transverse momentum of the selected lepton is required to be back-to-back with the E_T^{miss}. The main background contributions are related to SM production of W-boson and diboson. No significant excess is observed and therefore limits are calculated considering the transverse mass spectrum: $M_T = \sqrt{2 \cdot p_T^{\ell} \cdot E_T^{miss} \cdot (1 - \cos \Delta\varphi_{\ell,\nu})}$ with $\ell = e, \mu$ and $\Delta\varphi_{\ell,\nu}$ the azimuthal angle difference between lepton and missing energy in the transverse plane.

The transverse mass spectrum observed at $\sqrt{s} = 8$ TeV in the electron channel is shown in Fig. 3.

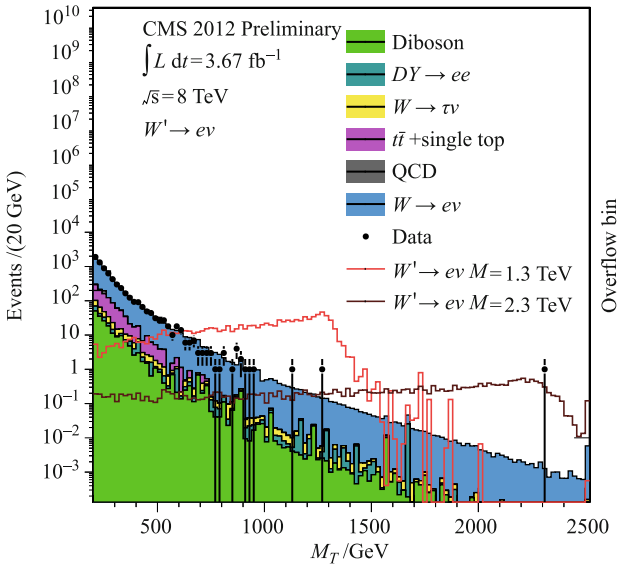

Fig. 3 The transverse mass distribution observed in the electron channel at $\sqrt{s} = 8$ TeV. The Monte Carlo simulated signal events are overlaid.

The SM background contributions normalized to their cross-section show that there is no significant excess in data. The calculated limit can be seen in Fig. 4 and for the combined statistics at 7 and 8 TeV centre of mass energy one can exclude W'_{MSSM} with a mass of less than 2.85 TeV at 95% C.L.. For masses below 1.4 TeV also the second Kaluza–Klein excitation can be excluded for a bulk mass parameter, μ, of 0.05 TeV, while a mass bellow 3.3 TeV is excluded for $\mu = 10$ TeV.

3 Heavy neutrino

One of the driving reasons for looking for physics beyond SM is the observation of the neutrino oscillation [17]. This implies that they are massive, while the SM assumes

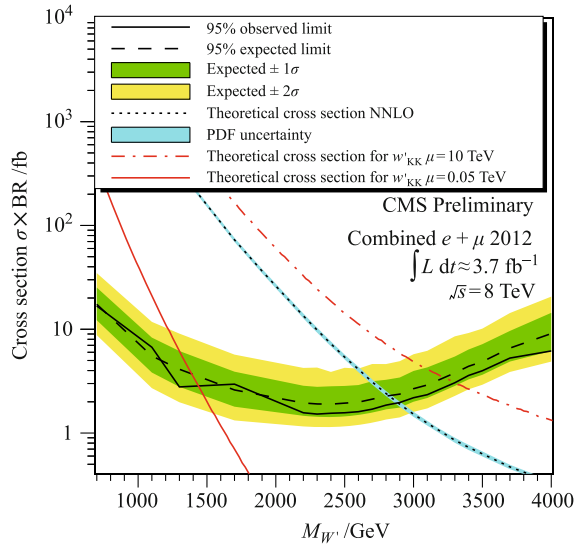

Fig. 4 The upper limits on the cross-section times branching fraction for W'_{SSM} production as a function of its mass.

that they are massless. The neutrino mass can be accommodated extending the SM by adding massive right-handed neutrinos [18]. The decay mode that is searched for is: $W'_R \to \ell_1 N_\ell \to \ell_1 \ell_2 W_R^* \to \ell_1 \ell_2 q q' \to \ell_1 \ell_2 jj$ with $\ell = e, \mu$, N_ℓ the heavy neutrino, W_R^* is off-shell and j a reconstructed jet. Therefore events with 2 leptons and at least 2 jets are selected.

The leading lepton is selected if the p_T is larger than 60 GeV, while the sub-leading lepton and the jets are required to have p_T greater than 40 GeV. Due to the large mass expected for W'_R, the signal can be enhanced relative to SM background contributions by selecting only events with dilepton invariant mass above 200 GeV and the invariant mass of the dilepton and dijets system above 600 GeV [19].

The main contributions from the SM background processes are given by the $t\bar{t}$ and Drell–Yan as one can observe in Fig. 5. Other contributions from W, single t and diboson production are also considered. No signal excess was observed and exclusion limits for various flavours of the heavy neutrino were calculated. In Fig. 6 the limit in the N_ℓ and W'_R mass plane is shown for the case when all flavours are considered.

Another search in the neutrino sector is for heavy Majorana neutrino. The small neutrino mass could be explained by introducing a new massive neutrino state: $m_\nu \approx y_\nu^2 v^2 / m_N$ where y_ν is ν Yukawa coupling to Higgs field and v the SM Higgs vacuum expectation, the "see-saw" mechanism. The investigated decay channel [20] is $q\bar{q} \to W^{\pm} \to N\ell^{\pm} \to W^{\mp}\ell^{\pm}\ell^{\pm} \to q\bar{q}\ell^{\pm}\ell^{\pm}$ with $\ell = e, \mu$. Events with only two same sign leptons with $p_T > 20$ and 10 GeV, at least two jets with p_T larger than 30 GeV and E_T^{miss} less than 50 GeV are selected.

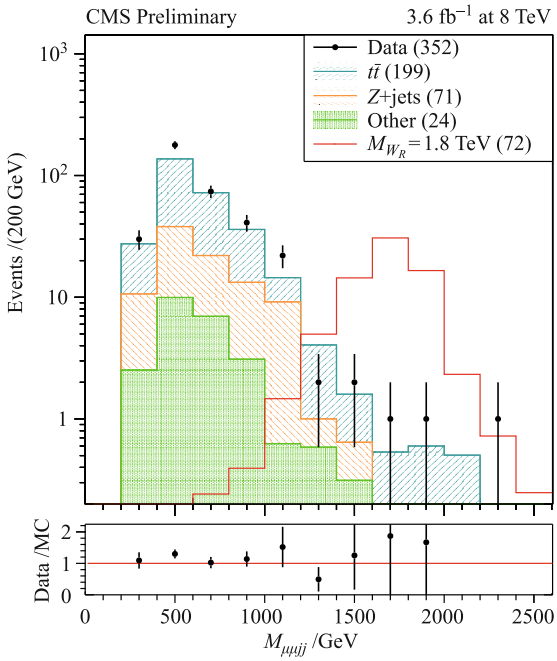

Fig. 5 The four object mass distribution for $\mu\mu jj$ events at $\sqrt{s} = 8$ TeV. The Monte Carlo simulated signal corresponds to a 1800 GeV W_R' and 900 GeV N_ℓ.

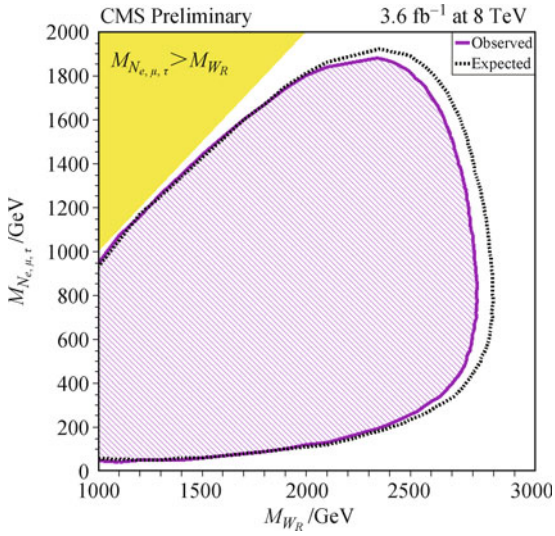

Fig. 6 The excluded region in N_ℓ and W_R' mass plane with $M_{N_\ell} = 1/(2M_{W_R})$ obtained considering electron, muon and tau flavour.

In this search, limits on the Majorana neutrino mixing elements are calculated. In Fig. 7 the exclusion limit on $|V_{\mu N}|$ is shown as function of M_N. For a 90 GeV Majorana neutrino the limits on the mixing elements are $|V_{\mu N}|^2 < 0.07$ and $|V_{eN}|^2 < 0.22$.

4 The 4$^{\text{th}}$ generation

The mass of a fourth generation quarks, t and b, is restricted to be greater than 350 GeV from direct searches

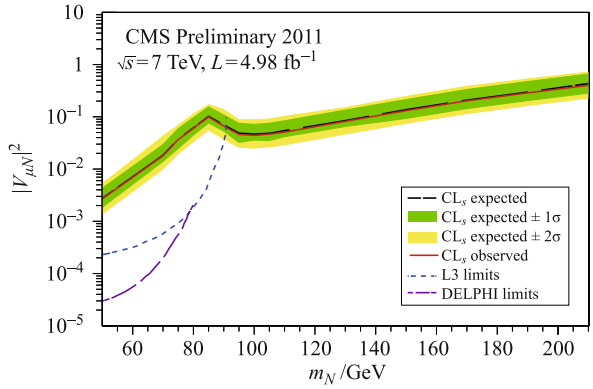

Fig. 7 The 95% C.L. exclusion region of $|V_{\mu N}|^2$ vs. the Majorana neutrino mass. The expected (*dashed black line*) and observed limit (*solid red line*) overlap.

[21]. The indirect search from LEP excludes a fourth light neutrino type [22]. The search for t' quark is performed in events where a pair of heavy top-like quarks are produced $t'\bar{t}' \to bW^+\bar{b}W^- \to b\ell^+\nu\bar{b}\ell^-\bar{\nu}$ with $\ell = e, \mu$.

Events triggered with two opposite-sign isolated leptons, e^+e^-, $e^\pm\mu^\mp$ or $\mu^+\mu^-$, with $p_T > 20$ GeV are selected. In addition, top-like events are enhanced by requiring two b-tagged jets with $p_T > 30$ GeV, while the Drell–Yan events are rejected by applying the $E_T^{miss} > 30$ GeV cut. The selected leptons and b-tagged jets are combined and from all invariant mass combinations, $M_{\ell b}$, the minimal one is chosen to look for the $t'\bar{t}'$ signal [23]. The presence of the signal is expected to be dominant for $M_{lb}^{min} > 170$ GeV as it is illustrated in Fig. 8 for a t' mass of 450 GeV. The main background contribution comes from the Standard Model $t\bar{t}$ (dilepton channel) production. Also other backgrounds as diboson and single top production were considered.

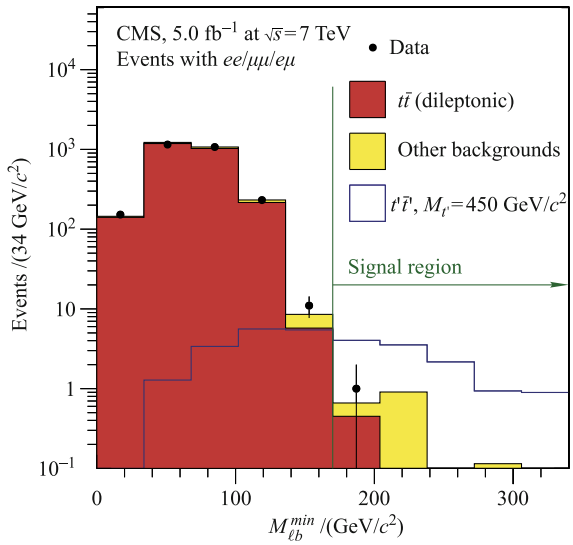

Fig. 8 The minimal invariant mass observed for the ℓb pairs combinations. The signal prediction for a 450 GeV t' is also shown.

The total SM background prediction in the signal region is 1.8 ± 1.1 events and only 1 event is observed in the analysed data. Because there is no evidence for an excess of events above SM expectations exclusion limits are calculated on the $t'\bar{t}'$ pair production cross section as shown in Fig. 9. At 95% C.L. the existence of a t' quark with a mass of 557 GeV is excluded.

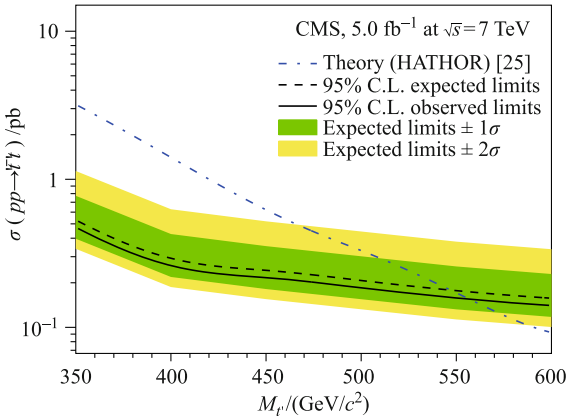

Fig. 9 The 95% C.L. upper limits on the production cross section of $t'\bar{t}'$ as a function of t' mass.

Also an inclusive search for quarks of the 4^{th} generation was performed [24]. In this search the limits on the masses of the t' and b' were calculated as a function of the CKM matrix element $|V_{tb}|$. The lower limit of $|V_{tb}| > 0.81$ obtained from the single t production cross section measurements [25] translate in a lower limit above 0.66 on the mixing between the third and fourth-generation quarks in this model, $|V_{t'b'}|^2$.

The $t\bar{t}$-like events are enhanced by requiring that the leading lepton, $p_T > 40$ GeV, is accompanied by two jets with p_T above 30 GeV, at least one of them being b-tagged, and $E_T^{miss} > 40$ GeV.

In order to discriminate between SM background contributions and the 4^{th} generation signal, the scalar sum on the transverse momenta on the final state reconstructed objects, S_T, is used: $S_T = E_T^{miss} + p_T^{\ell} + p_T^{b} + p_T^{j} + \sum_{i=0}^{N} p_T^{W^i_{q\bar{q}}}$ where $p_T^{W^i_{q\bar{q}}}$ is the transverse momentum of the i^{th} reconstructed hadronically decaying W-boson.

The observed scalar sum S_T in events where both jets are b-tagged and the prediction from SM background processes is presented in Fig. 10. The expected signal contribution from 550 GeV 4^{th} generation quarks is also shown. No excess over the expected SM predictions was observed, therefore limits for $m_{b'} = m_{t'}$ as function of $|V_{tb}|^2 = |V_{t'b'}|^2$ were calculated. In Fig. 11 it can be seen that 4^{th} generation quarks with mass below 685 GeV are excluded at 95% C.L..

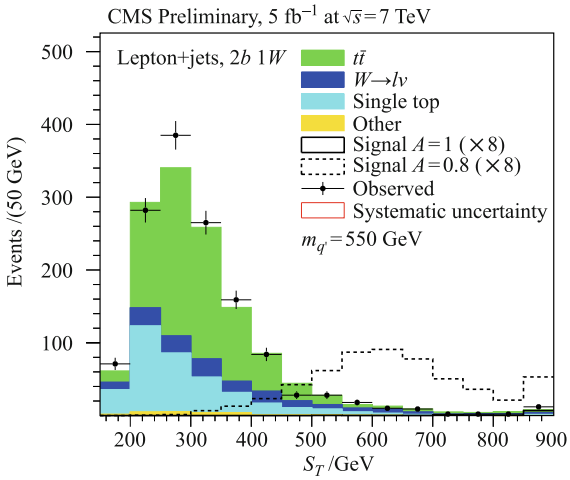

Fig. 10 The S_T distribution in events where both jets are b-tagged and the Standard Model expectations. The signal distribution is shown for two values of $|V_{t'b'}|^2$ and for b' and t' masses of 550 GeV. The signal is magnified by a factor of 8 for visibility purposes, while last bin includes the overflow.

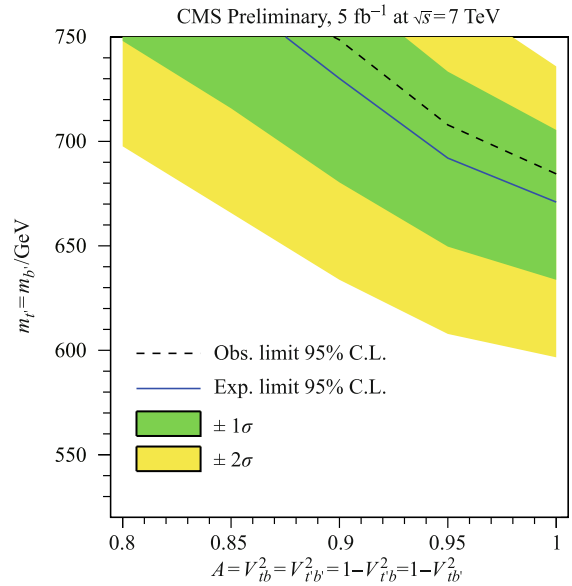

Fig. 11 The exclusion limits on $m_{b'} = m_{t'}$ as function of $|V_{tb}|^2 = |V_{t'b'}|^2$. The parameter values below the line are excluded at 95% C.L..

5 Excited leptons

One attempt to explain the three generation structure of the fermion families leads to models where quarks and leptons can be postulated as being composed of "more" fundamental constituents, the preons [26]. These excited fermions are supposed to couple to the SM fermions therefore they can be produced via contact interaction and one of the possible decays is radiative through the emission of a photon. The signal $\ell^{\pm}\ell^{*\mp} \rightarrow \ell^{\pm}\ell^{\mp}\gamma$ is searched with $\ell = e, \mu$.

The events selected for this search have two isolated leptons and one photon. In case of electrons it is required

that their p_T is greater than 35 GeV in the barrel region, $|\eta| < 1.4442$, and 45 GeV in the end-caps. The muons are selected in the $|\eta| < 2.1$ region with $p_T > 45$ and 40 GeV, for the leading and sub-leading one, respectively. The photon selection ensures a high energy resolution and purity for $E_T > 35$ GeV in the barrel region. It is also well separated in η and φ from the reconstructed muons and electrons by requiring a radius between its direction and the leptons of 0.7 and 0.5, respectively. The invariant mass of each lepton and the photon, $M_{\ell\gamma}$, is analysed in the $(M_{\ell\gamma}^{max}, M_{\ell\gamma}^{min})$ plane [27]. This approach allows us to enhance the signal in an L-shape region as shown in Fig. 12 for an excited lepton of 0.2 TeV.

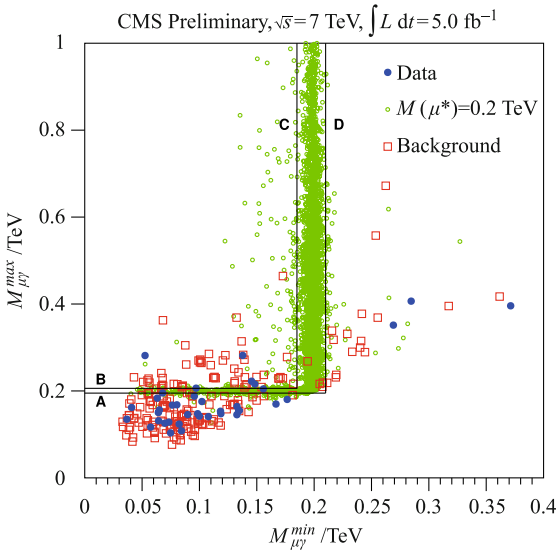

Fig. 12 The $M_{\ell\gamma}^{max}$ vs. $M_{\ell\gamma}^{min}$ distribution for the excited muon analysis. The data are illustrated with blue plain circles, background contributions with red squares and the expected signal for an excited muon of 0.2 TeV.

Upper limits on the production cross section of the excited leptons are calculated at 95% C.L. using a single bin counting method and are presented in Fig. 13.

For excited electrons (muons) with masses between 0.6 and 2 TeV production cross sections higher than 1.57–1.32 fb (1.30–1.14 fb) are excluded. The limits are more stringent, 0.73–0.60 fb, for models where $M_{e^*} \approx M_{\mu^*}$. Also, for the scale of contact interaction $\Lambda = M_{\ell^*}$ excited electrons (muons) with masses below 1.9 TeV are excluded.

6 Gauge-mediated symmetry breaking

Some of the models predicting the physics beyond SM, for example hidden valley scenarios [28] or supersymmetry with gauge-mediated symmetry breaking (GMSB) [29], predict long lifetime particles that may be neutral and decay into photon and weakly interacting particles.

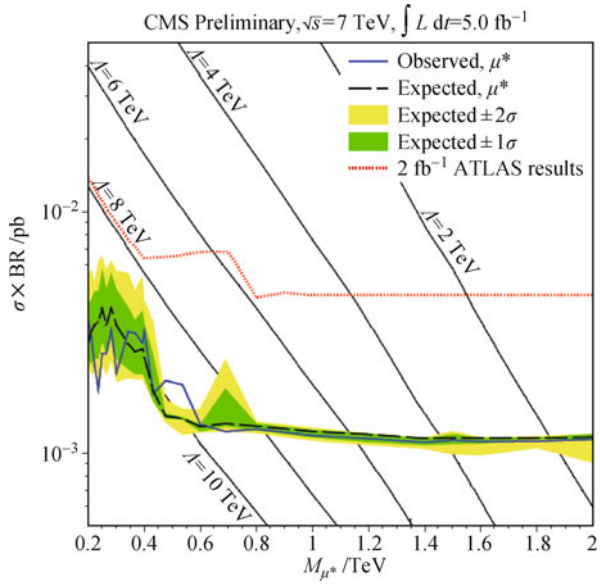

Fig. 13 The 95% C.L. expected and observed upper limit on cross-section production of excited muons. For different Λ scales, the excited lepton leading-order cross-section are shown with the black solid lines.

One example is the neutralino which decays into a photon and a weakly interacting gravitino: $\widetilde{\chi}_1^0 \to \gamma\widetilde{G}$.

The event signature is therefore given by an excess in the E_T^{miss} and displaced photon signals. The time of impact of the photon on the surface of the ECAL and ECAL cluster shape are most important discriminating

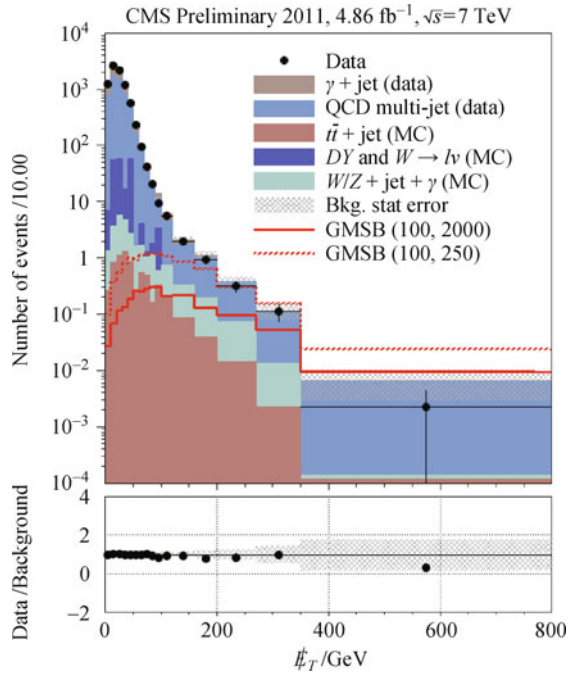

Fig. 14 The E_T^{miss} spectrum at $\sqrt{s} = 7$ TeV. The multi-jet and γ+jet backgrounds use shape derived from data. The rest of the background contributions are estimated using Monte Carlo simulation and normalized according to their cross-sections. The signal corresponds to the SUSY breaking scale $\Lambda = 100$ TeV and the decay length $c\tau = 2000$ or 250 mm.

variables in this search [30]. The photon is selected in the $|\eta| < 1.4$ region with $E_T > 100$ GeV. Together with the photon also three jets are required with $p_T > 35$ GeV. In the E_T^{miss} spectrum, at large values, an excess of events is predicted by the model as illustrated in Fig. 14

No excess of events was observed and the exclusion limits on the decay length of neutralino as a function of its mass, presented in Fig. 15, were calculated. The $\widetilde{\chi}_1^0$ mass upper limit goes up to 220 GeV, while the $c\tau$ limit up to 6000 mm.

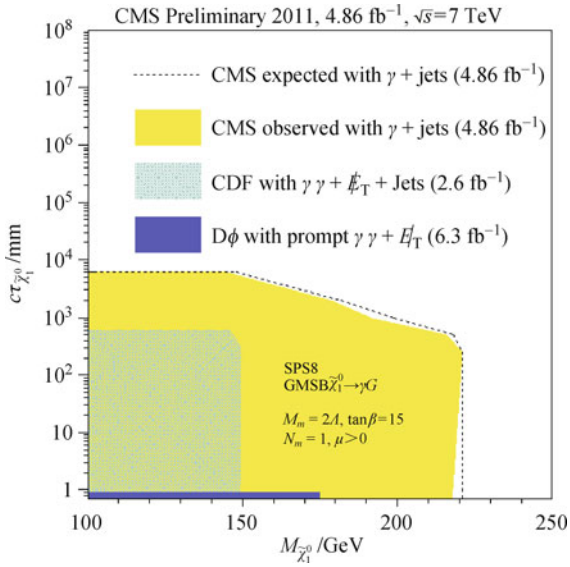

Fig. 15 The observed and expected exclusion region of the $\widetilde{\chi}_1^0$ proper decay length and mass.

7 Lepto-quarks

Grand Unified Theories, composite models [31], technicolor schemes [32] and superstring-inspired E6 models [33] predict the existence of leptoquarks, particles which carry both baryon and lepton number. The dominant production mechanisms of the leptoquarks are foreseen to be gluon-gluon fusion and $q\bar{q}$ annihilation.

The channel used in the search of the first [34] and second [35] generation of leptoquarks is $LQ\overline{LQ} \to \ell q \ell q(\nu q)$ with $\ell = e, \mu$. The signal events are characterised by two energetic leptons, two jet and a large scalar sum S_T. For example in the $\mu\mu jj$ channel muons with $p_T > 40$ GeV and jets with p_T larger than 30 GeV are selected. In addition a cut on $S_T > 250$ GeV is applied. The analysis is optimised using the smallest muon-jet invariant mass that minimize the $M_{LQ} - M_{\overline{LQ}}$ difference.

In Fig. 16 the invariant mass $M_{\mu j}$ is shown after the final selection. The main SM background contributions in the final distribution of the $\mu\mu jj$ channel are given by the Drell–Yan and $t\bar{t}$. Other contributions as W-boson, diboson and QCD multijet production processes are also considered. The number of events observed in data is consistent with the SM background prediction. Therefore an upper limit on the leptoquarks production cross section times the square of the branching ratio, $\beta = BR(LQ \to \ell q)$, was calculated.

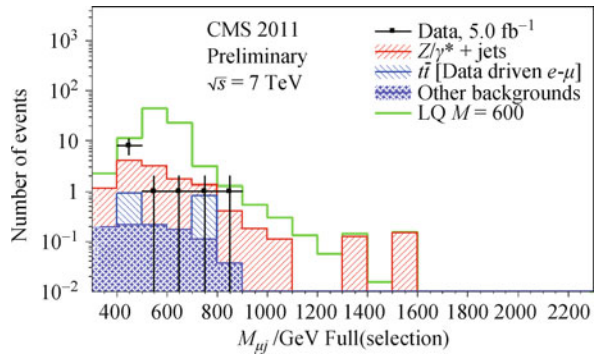

Fig. 16 The muon-jet invariant mass distribution after the final selection. The signal prediction for a leptoquark mass of 550 GeV in the $\mu\mu jj$ channel is also illustrated.

For the second generation leptoquarks the exclusion limits are shown in Fig. 17.

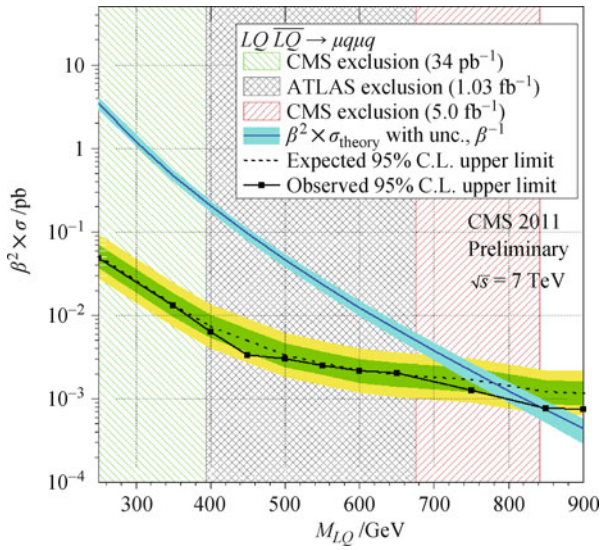

Fig. 17 The upper limit at 95% C.L. on the leptoquarks production cross section times the square of the branching ratio, β, as a function of the second generation leptoquarks mass. For $\beta = 1$ also the theoretical scalar leptoquarks production cross section and its uncertainties are shown.

The pair production of the first generation leptoquarks is excluded at 95% C.L. for masses below 830 (640) GeV for $\beta = 1(0.5)$. The second generation leptoquarks pair production is excluded at 95% C.L. for masses below 632 (523) GeV for $\beta = 1(0.5)$.

The search for the third generation leptoquarks was done with the channel $LQ\overline{LQ} \to \tau b \tau b \to \ell \tau_{had} b\text{-}jet\ b\text{-}jet$ where $\ell = e, \mu$ and τ_{had} is tau-lepton decaying fully hadronic [36]. The selected events have an electron

(muon) with the p_T greater than 30 GeV and a hadronic decaying tau with $p_T > 50$ GeV. The signal prediction against the Drell–Yan contribution is enhanced requiring two b-tagged jets with $p_T > 30$ GeV. An additional discrimination against the background is obtained when applying $M(\tau_h, b\text{-}jet) > 170$ (190) GeV for signal with masses up to 450 GeV (greater than 450 GeV). The $M(\tau_h, b\text{-}jet)$ is chosen such that the $M_{\ell b} - M_{\tau_h, bjet}$ is minimized. The S_T distribution, where $S_T = p_T^{\tau_h} + p_T^{\ell} + p_T^{bjet_1} + p_T^{bjet_2}$, after final selection is used to search for the third generation leptoquarks. In Fig. 18 one can observe that no excess of events is seen with respect to SM background predictions.

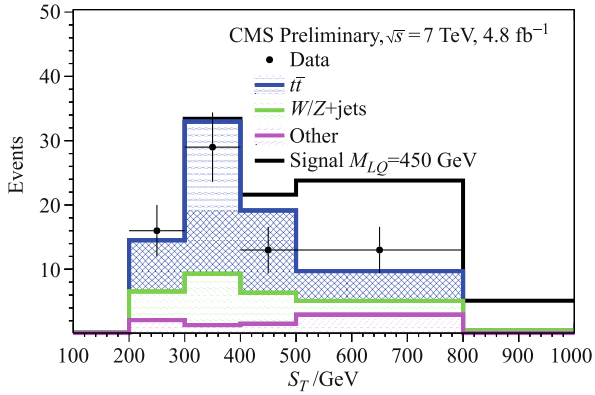

Fig. 18 The S_T distribution observed in data and the Standard Model background predictions normalized according to their cross-sections. The signal (*black line*) after $M(\tau_h, b\text{-}jet) > 170$ GeV is also illustrated.

The stop decaying via $\tilde{t_1} \to \tau b$ has the same event signature. Therefore exclusion limits can be calculated for the third generation leptoquarks pair production as well as for the stop pair production as it can be seen in Fig. 19.

The existence of the third generation leptoquarks with masses below 535 GeV is excluded at 95% C.L. for a branching ratio to τb of 100%. The vector leptoquarks with masses below 760 GeV are also excluded. The stop masses below 240 GeV are excluded for any value of the λ'_{333} coupling [37] to τ-lepton and b-quark. For $\lambda'_{333} = 1$ stops with masses below 453 GeV are excluded at 95% C.L..

8 Extra-dimensions and other searches

The Randall-Sundrum (RS) model [38] predicts an effective theory where the graviton propagates in a 5^{th} extra dimension. This could lead to Kaluza–Klein tower of states that can be detected as massive spin 2 resonances, e.g. the RS graviton G^*. The model can be described phenomenologically with the graviton mass and the ratio of the 5th dimensional curvature to the reduced Plank

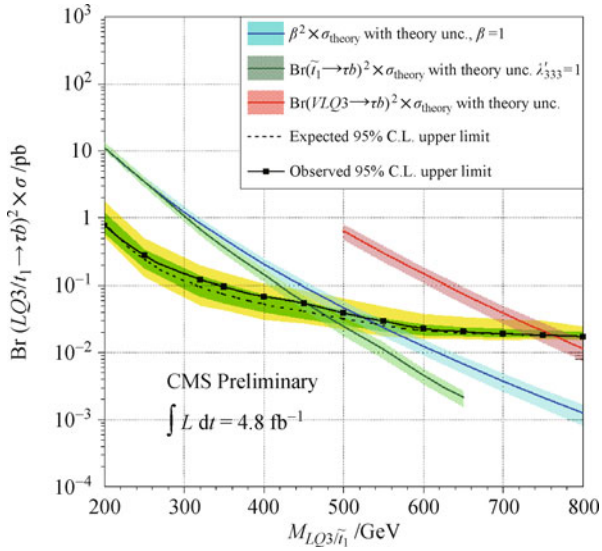

Fig. 19 The 95% C.L. limits on third generation leptoquarks pair production cross-section times the branching ratio to decay into τb as a function of leptoquark mass. Because $\tilde{t_1} \to \tau b$ has the same event signature also the limit for the stop pair production is calculated.

mass ($k/M_{\rm Plank}$), the coupling constant of the model.

The final state searched for the existence of the RS graviton $G^* \to Z^0 Z^0 \to q\bar{q}\nu\bar{\nu}$ is described by large E_T^{miss} and only 2 jets [39]. The leading jet is required to have a $p_T > 200$ GeV and a mass larger than 70 GeV. In order to veto the QCD multijet background events the two jets have to be well separated in the azimuthal angle, $\Delta\varphi > 2.8$. The W-boson SM contribution is reduced by removing events with isolated electrons or muons. The signal is further enhanced by selecting events with jet-E_T^{miss} transverse mass $M_T^G = \sqrt{2p_T^{\rm jet} E_T^{miss} \left[1 - \cos\Delta\varphi({\rm jet}, E_T^{miss})\right]}$ greater than 900 GeV and $E_T^{miss} > 300$ GeV.

In Fig. 20 the jet-E_T^{miss} transverse mass is presented. The main SM background contributions are given by the processes $Z^0 + nq \to \nu\bar{\nu} + n$jets and $W + nq \to \ell\nu + n$jets. The expected signal contribution for $M_{G^*} = 1250$ GeV and $k/M_{\rm Plank} = 0.2$ is also shown.

No excess of events was observed. Limits at 95% C.L. on the cross-section production times the branching ratio for a resonance decaying in $Z^0 Z^0$ and consequently into a massive jet plus E_T^{miss} were calculated.

For a mass between 1000 and 1500 GeV, they are found to be between 0.047 and 0.021 pb. From the perspective of the RS model it can be concluded that the RS graviton is excluded for $k/M_{\rm Plank}$ above [0.11, 0.29] as it can be seen in Fig. 21.

Another search where the hypothesis of existence RD Graviton can be tested is the investigation of the dijet invariant mass spectrum [40]. Many models with a final state with $q\bar{q}$, qq, $\bar{q}\bar{q}$, qg and/or gg can be probed in this

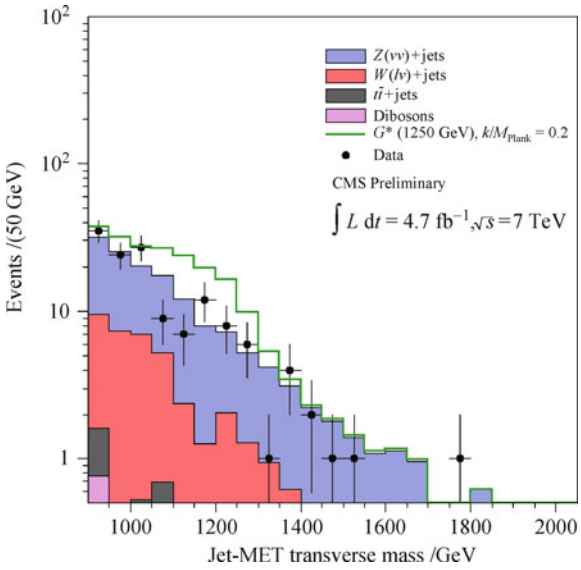

Fig. 20 The jet-E_T^{miss} transverse mass observed in $\sqrt{s} = 7$ TeV data and the Standard Model background predictions. The expected signal for $M_{G^*} = 1250$ GeV and $k/M_{\rm Plank} = 0.2$ is also presented.

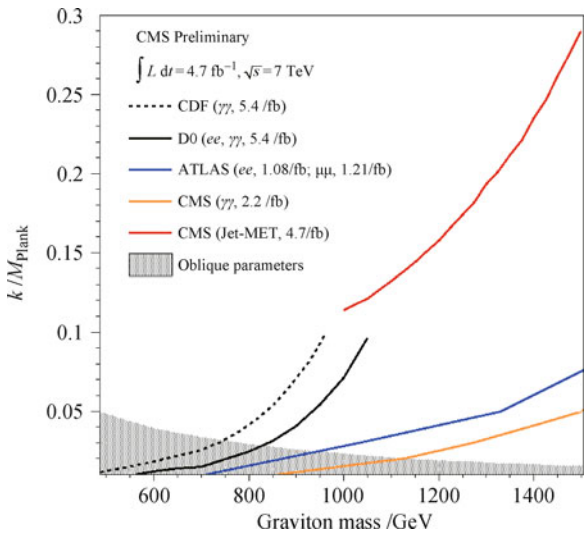

Fig. 21 The exclusion limits interpreted in the Randall–Sundrum model for $G^* \to Z^0 Z^0 \to q\bar{q}\nu\bar{\nu}$.

search. Events with jets in $|\eta| < 2.5$ region with $p_T > 30$ GeV are selected. The selected jets are combined into wide jets [41, 42] that are used afterwards to measure the dijet mass spectrum. The two wide jets are required to be close in η, $\Delta\eta_{jj} < 1.3$, and have $M_{jj} > 890$ GeV. In Fig. 22 the dijet mass spectrum is presented for the data collected at $\sqrt{s} = 8$ TeV. Expected contributions from a W'-boson with 1.5 TeV mass and for E_6 scalar diquark [43] with 3.5 TeV are also presented.

No excess was observed, exclusion limits were calculated on the cross section times branching ratio and acceptance.

These limits are compared with predictions from various models in Fig. 23.

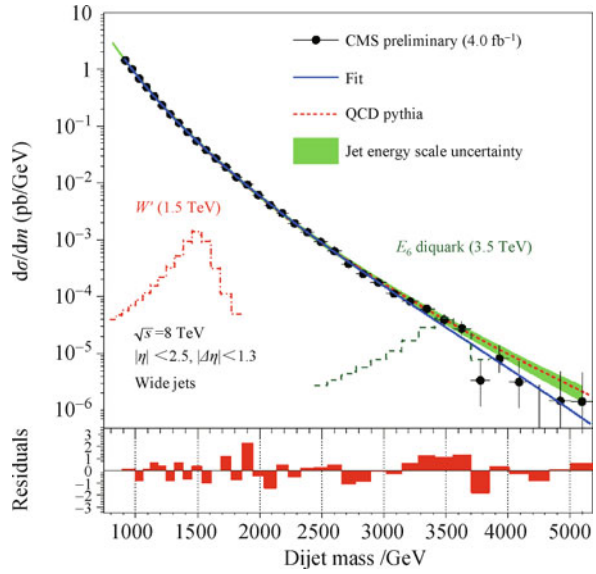

Fig. 22 Dijet mass spectrum from wide jets together with expected signal contributions for a 1.5 TeV W'-boson and 3.5 TeV E_6 scalar diquark.

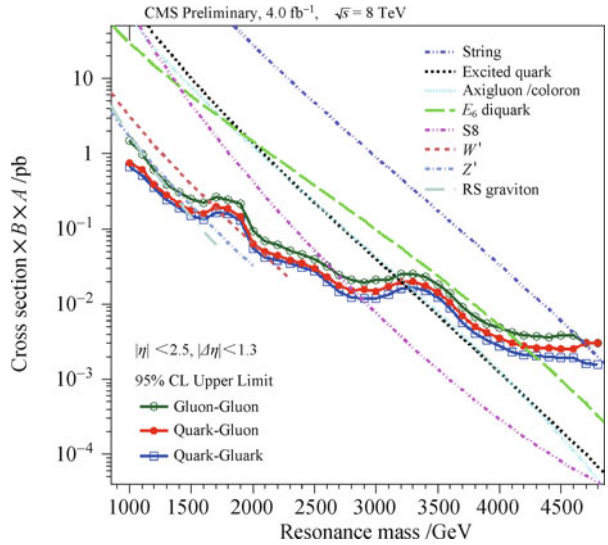

Fig. 23 The observed upper limits at 95% C.L. on the cross section times branching ratio and acceptance for gluon-gluon (*open circles*), quark-gluon (*solid circles*), and quark-quark (*open boxes*) resonances. The expectation for string resonances [44], E6 diquarks, excited quarks [45], axigluons [46], colorons [47], s8 resonances [48], W' and Z' new gauge bosons, and Randall-Sundrum gravitons are also presented.

Motivated by the hierarchy problem, the ADD model [50] with n extra spatial dimensions predicts production of microscopic black hole (BH) in proton-proton collisions at the high energies. These BH do not grow like cosmics black holes, but rather evaporate.

The event signature is given by a large number of energetic final state particles where 75% are jets. Therefore events with isolated energetic leptons, $p_T > 50$ GeV, isolated photons with $E_T > 50$ GeV and at least 2 jets with $p_T > 50$ GeV in $|\eta| < 2.6$ region are selected.

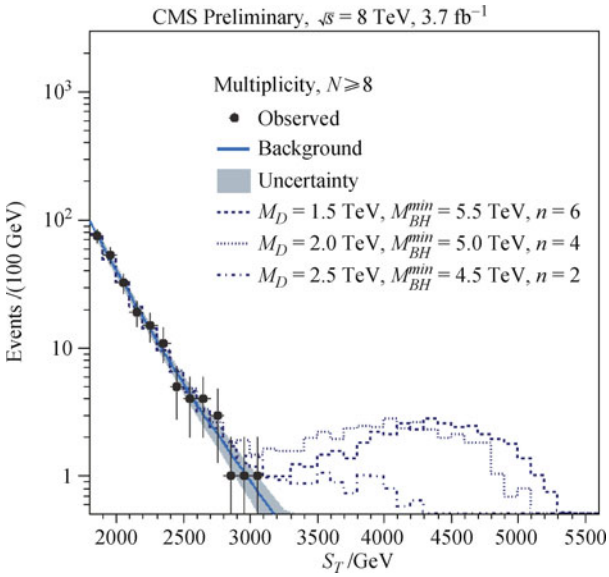

Fig. 24 The scalar sum on the transverse momenta and missing energy, S_T, for events with a multiplicity of at least 8 energetic objects. The solid line with error bands illustrates the background prediction. Expected signal contributions are given for certain number of extra dimensions, n, multidimensional Planck scale, M_D, and the minimum black hole mass, M_{BH}^{min}.

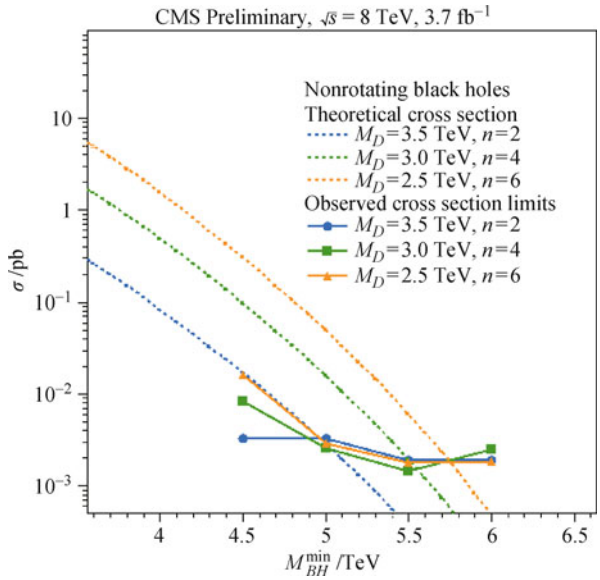

Fig. 25 The observed cross section limits at 95% C.L. using counting experiments for various black hole parameter sets. The signal predicted cross sections with the BLACKMAX generator [51] are also shown.

The discriminating variable chosen in this search [49] is the scalar sum on the transverse momenta on the final state reconstructed objects, S_T, which goes over all jets, leptons, photons with $p_T > 50$ GeV and $E_T^{miss} > 50$ GeV.

The observed data are in agreement with the expected QCD multijet background contribution and cross section limits at 95% C.L. can be extracted for various BH parameter sets, as shown in Fig. 25.

The ADD model can be also tested looking at the presence of the tower Kaluza–Klein excitations of the graviton. These would lead to an enhancement of the fermion and boson pair production cross sections, especially at high energies. A search in the dielectron mass spectrum was performed [52] with the data collected at $\sqrt{s} = 7$ TeV.

The event selection requires two isolated electrons with p_T greater than 35 GeV in the barrel region and 40 GeV in the endcap region. An optimized invariant mass cut, $M_{ee} > 1.3$ TeV, to the expected sensitivity was used.

In Fig. 26 the observed dielectron invariant mass spectrum is presented. The dominant SM background contribution is given by the Drell–Yan process. The expected enhancement of events from the ADD model with $\Lambda_T = 3.0$ TeV, the model unknown parameter related to the number of extra dimensions, is also shown. There is one event observed for $M_{ee} > 1.3$ TeV, while 0.79 ± 0.15 events are expected from the SM prediction.

In Fig. 27 the exclusion limits at 95% C.L. on the cross

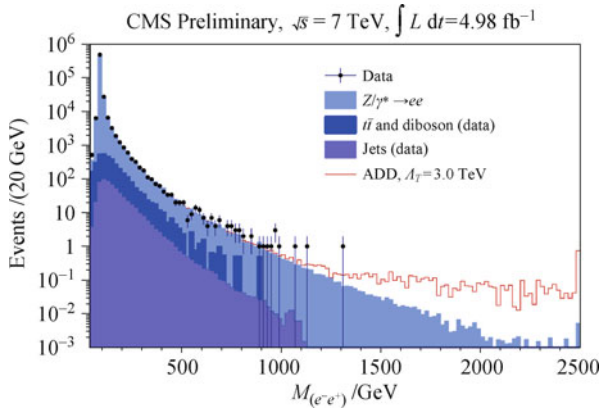

Fig. 26 The measured dielectron invariant mass spectrum and the estimated standard model background contributions. The signal expected from the ADD model for $\Lambda_T = 3.0$ TeV is also displayed.

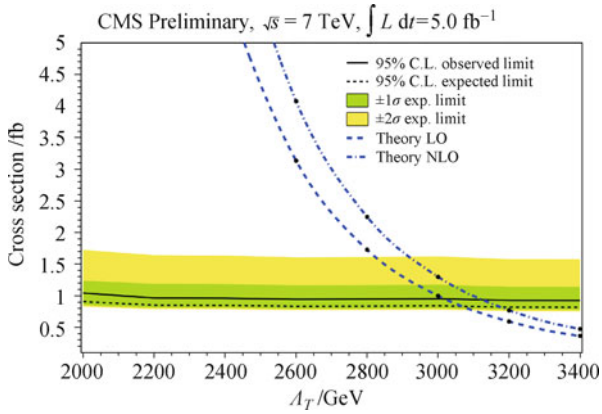

Fig. 27 The 95% C.L. limits on the cross section of an ADD signal with a dielectron pair in the final state. The expected leading-order and next-to-leading-order cross section are also illustrated.

section of an ADD signal that decays into a dielectron pair are shown together with the leading-order and next-to-leading-order theoretical predictions. A similar search using the dimuon final state was also performed [53].

Another test of the ADD model was performed on events containing a single energetic jet (monojet) and large E_T^{miss}. These events are signature of direct production of a graviton produced via processes as $gg \rightarrow gG$. The same event signature corresponds also the best candidate for dark matter (DM), a stable weakly interactive particle χ. The DM particles could be produced at the LHC if their mass is less than half of the parton centre-of-mass energy. The interaction with the SM particle can be seen as a contact interaction at the scale Λ. In this search χ is assumed to be a Dirac fermion.

Events selected for this search [54] have one jet with p_T larger than 110 GeV and $E_T^{miss} > 200$ GeV. The signal is enhanced with respect to SM background contributions by applying a lepton veto, no muon or electron with $p_T > 10$ GeV, and no more than 2 jets with $p_T > 30$ GeV.

In Fig. 28 the E_T^{miss} spectrum is shown together with examples of ADD and DM signals. The observed number of events is consistent with the SM prediction. Exclusion limits on the dark matter-nucleon scattering cross section were calculated for spin independent and depended models, as shown in Fig. 29.

The lower limit at 95% C.L. on the multidimensional Plank scale M_D in the ADD model is presented in Fig. 30.

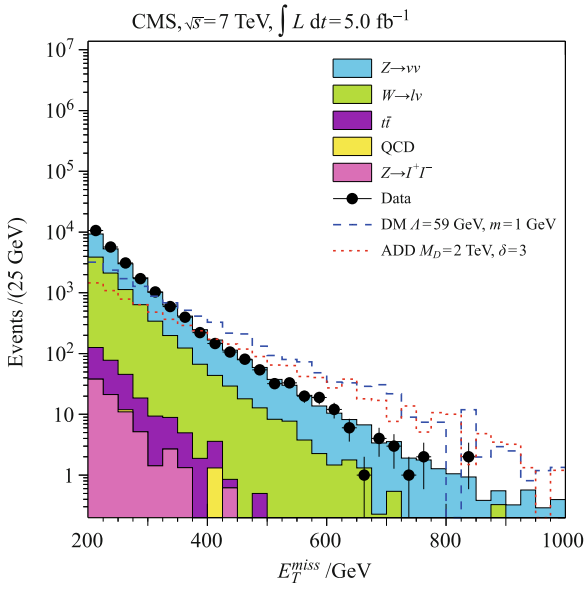

Fig. 28 The observed E_T^{miss} spectrum and the SM background contributions. Signal expectation for a dark matter particle at the scale $\Lambda = 599$ GeV, axial-vector couplings and $M_\chi = 1$ GeV, as well as expectation for an ADD signal with the multidimensional Plank scale $M_D = 2$ TeV and $\delta = 3$ extra dimensions are also presented.

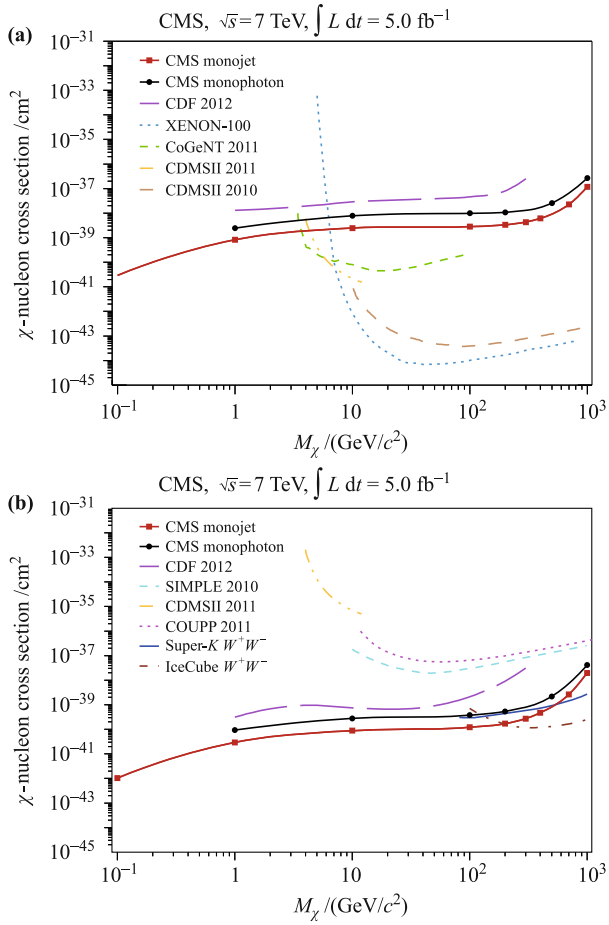

Fig. 29 The 90% C.L. upper limits on the dark matter-nucleon scattering cross section for spin independent **(a)** and spin dependent **(b)** models using monojet final state. For comparison, results from the monophoton final state search [55] as well as from other experiments are also shown.

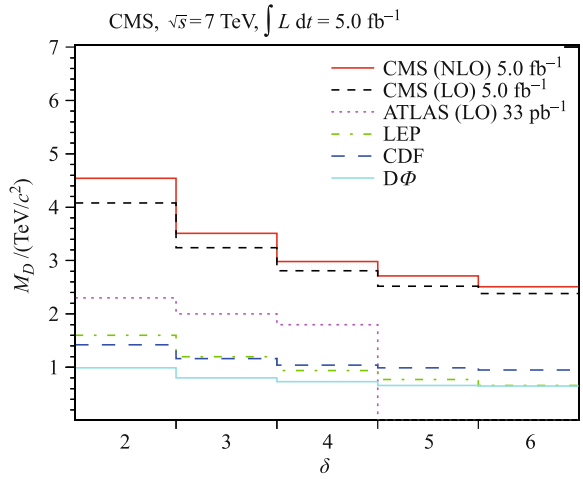

Fig. 30 The lower limits at 95% C.L. on the multidimensional Plank scale M_D as a function of δ extra dimensions.

9 Conclusions

In this paper results on the searches for physics beyond

the standard model (SM) in pp collisions at $\sqrt{s} = 7$ and 8 TeV recorded with the CMS experiment were presented. The analyses performed with dedicated physics objects were focused on specific final states topologies. In this way various theoretical models could be tested comparing their prediction for a certain final state. No significant excess of events has been observed so far, therefore new limits were set on the cross section production of the new gauge Z'- and W'-bosons, heavy neutrino, quarks of the 4^{th} generation, leptoquarks as well as of the signal predicted by models considering extra dimensions and dark matter.

Although many final states topologies were tested, most of them refer to phase-space regions where the standard model processes contributions is highly suppressed. It is time to extend these searches also in regions of phase-space where the precision needs to be improved in order to better discriminate with respect to contributions from the SM processes.

References and notes

1. I. Aitchinson, arXiv: hep-ph/0505105, 2005
2. S. Martin, arXiv: hep-ph/9709356, 1997
3. CMS Collaboration, The CMS experiment at the CERN LHC, Journal of Instrumentation, 3, S08004
4. CMS Collaboration, Performance of CMS muon reconstruction in pp collision events at $\sqrt{s} = 7$ TeV, Journal of Instrumentation, 7, P10002
5. CMS Collaboration, Electron reconstruction and identification at $\sqrt{s} = 7$ TeV, CMS-PAS-EGM-10-004
6. CMS Collaboration, Study of tau reconstruction algorithms using pp collisions data collected at $\sqrt{s} = 7$ TeV, CMS-PAS-PFT-10-004
7. CMS Collaboration, Particle-flow event reconstruction in CMS and performance for jets, Taus and MET, CMS-PASPFT-09-001
8. CMS Collaboration, b-jet identification in the CMS experiment, CMS-PAS-BTV-11-004
9. M. Cacciari, G. P. Salam, and G. Soyez, J. High Energy Phys., 2008, 0804: 063, arXiv: 0802.1189
10. M. Cacciari and G. P. Salam, Phys. Lett. B, 2007, 659(1–2): 119
11. G. Altarelli, B. Mele, and M. Ruiz-Altaba, Z. Phys. C, 1989, 45(1): 109
12. A. Leike, Phys. Rep., 1999, 317(3–4): 143, arXiv: hep-ph/9805494
13. CMS Collaboration, Search for resonances in the dilepton mass distribution in pp collisions at $\sqrt{s} = 8$ TeV, CMS-PASEXO-12-015
14. C. R. Chen, M. M. Nojiri, S. C. Park, et al., J. High Energy Phys., 2009, 09: 078, arXiv: 0903.1971
15. K. Kong, S. C. Park, and T. G. Rizzo, J. High Energy Phys., 2010, 04: 081, arXiv: 1002.0602
16. CMS Collaboration, Search for leptonic decays of W' bosons in pp collisions at $\sqrt{s} = 8$ TeV, CMS-PAS-EXO-12-010
17. C. Giunti and M. Laveder, arXiv: hep-ph/0310238, 2003
18. W. Y. Keung and G. Senjanovic, Phys. Rev. Lett., 1983, 50(19): 1427
19. CMS Collaboration, Search for a heavy neutrino and righthanded W of the left-right symmetric model in pp collisions at 8 TeV, CMS-PAS-EXO-12-017
20. CMS Collaboration, arXiv: 1207.6079, CMS-PAS-EXO-11-076
21. CDF Collaboration, Phys. Rev. Lett., 2011, 106: 141803
22. D. Decamp, et al., Phys. Lett. B, 1989, 231: 519
23. CMS Collaboration, Search for a heavy top-like quark in the dilepton final state in pp collisions at 7 TeV, CMS-PASEXO-11-050
24. CMS Collaboration, Inclusive search for a sequential fourth generation of quarks, CMS-PAS-EXO-11-098
25. D0 Collaboration, arXiv: 1201.4156, 2012
26. H. Terazawa, M. Yasue, K. Akama, and M. Hayashi, Phys. Lett. B, 1982, 112(4–5): 387
27. CMS Collaboration, Search for excited leptons in 5 fb^{-1} of pp collisions at $\sqrt{s} = 7$ TeV with the CMS detector, CMS-PASEXO-11-034
28. M. J. Strassler and K. M. Zurek, Phys. Lett. B, 2007, 651(5–6): 374379, arXiv: hep-ph/0604261
29. G. F. Giudice and R. Rattazzi, Phys. Rep., 1999, 322(6): 419499, arXiv: hep-ph/9801271
30. CMS Collaboration, Search for long-lived particles using displaced photons in pp collisions at $\sqrt{s} = 7$ TeV, CMS-PASEXO-11-035
31. W. Buchmüller and D. Wyler, Phys. Lett. B, 1986, 177(3–4): 377
32. S. Dimopoulos, Nucl. Phys. B, 1980, 168(1): 69
33. V. Angelopoulos, J. Ellis, H. Kowalski, D. V. Nanopoulos, N. D. Tracas, and F. Zwirner, Nucl. Phys. B, 1987, 292: 59
34. CMS Collaboration, Search for pair production of first-generation scalar leptoquarks in pp collisions at $\sqrt{s} = 7$ TeV, CMS-PAS-EXO-11-027
35. CMS Collaboration, Search for second generation scalar leptoquarks, CMS-PAS-EXO-11-028
36. CMS Collaboration, Search for pair producti on of third generation leptoquarks and stops that decay to a tau and a b-quark, CMS-PAS-EXO-12-002
37. R. Barbier, et al., Phys. Rep., 2005, 420: 1
38. L. Randall and R. Sundrum, Phys. Rev. Lett., 1999, 83: 3370, arXiv: hep-ph/9905221
39. CMS Collaboration, Search for RS gravitons decaying into a jet plus MET, CMS-PAS-EXO-11-061
40. CMS Collaboration, Search for narrow resonances using the dijet mass spectrum in pp collisions at $\sqrt{s} = 8$ TeV, CMSPAS-EXO-12-016

41. M. Cacciari, J. Rojo, G. P. Salam, et al., J. High Energy Phys., 2008, 0812: 032, arXiv: 0810.1304
42. D. Krohn, J. Thaler, and L.-T. Wang, J. High Energy Phys., 2010, 02: 084
43. J. L. Hewett and T. G. Rizzo, Phys. Rep., 1989, 183(5–6): 193
44. S. Cullen, M. Perelstein, and M. E. Peskin, Phys. Rev. D, 2000, 62(5): 055012
45. U. Baur, I. Hinchliffe, and D. Zeppenfeld, Int. J. Mod. Phys. A, 1987, 2(04): 1285
46. P. H. Frampton and S. L. Glashow, Phys. Lett. B, 1987, 190(1–2): 157
47. E. H. Simmons, Phys. Rev. D, 1997, 55(3): 1678
48. T. Han, I. Lewis, and Z. Liu, J. High Energy Phys., 2010, 1012: 085, arXiv: 1010.4309
49. CMS Collaboration, Search for microscopic black holes at $\sqrt{s} = 7$ TeV with the CMS detector, CMS-PAS-EXO-12-009
50. N. Arkani-Hamed, S. Dimopoulos, and G. Dvali, Phys. Lett. B, 1998, 429: 263267, arXiv: hep-ph/9803315
51. D. C. Dai, C. Issever, E. Rizvi, G. Starkman, D. Stojkovic, et al., arXiv: 0902.3577, 2009
52. CMS Collaboration, Search for large extra dimensions in di-electron final state in 2011 pp collisions at $\sqrt{s} = 7$ TeV, CMS-PAS-EXO-12-023
53. CMS Collaboration, Phys. Lett. B, 2012, 711: 15, arXiv: 1202.3827
54. CMS Collaboration, Search for dark matter and large extra dimensions in monojet events in pp collisions at $\sqrt{s} = 7$ TeV, CMS-PAS-EXO-11-059
55. CMS Collaboration, Phys. Rev. Lett., 2012, 108: 261803, arXiv: 1204.0821